ACS Medicinal Chemistry Letters

pubs.acs.org/acsmedchemlett Letter

Discovery of Aminopyrazole Derivatives as Potent Inhibitors of Wild-Type and Gatekeeper Mutant FGFR2 and 3

Ryan A. Brawn,* Andrew Cook, Kiyoyuki Omoto, Jiyuan Ke, Craig Karr, Federico Colombo, Milena Virrankoski, Sudeep Prajapati, Dominic Reynolds, David M. Bolduc, Tuong-Vi Nguyen, Patricia Gee, Deanna Borrelli, Benjamin Caleb, Shihua Yao, Sean Irwin, Nicholas A. Larsen, Anand Selvaraj, Xuesong Zhao, and Stephanos Ioannidis

Cite This: https://dx.doi.org/10.1021/acsmedchemlett.0c00517 Read Online

ACCESS | Metrics & More | Article Recommendations | Supporting Information

ABSTRACT: Fibroblast growth factor receptors (FGFR) 2 and 3 have been established as drivers of numerous types of cancer with multiple drugs approved or entering late stage clinical trials. A limitation of current inhibitors is vulnerability to gatekeeper resistance mutations. Using a combination of targeted high-throughput screening and structure-based drug design, we have developed a series of aminopyrazole based FGFR inhibitors that covalently target a cysteine residue on the P-loop of the kinase. The inhibitors show excellent activity against the wild-type and gatekeeper mutant versions of the enzymes. Further optimization using SAR analysis and structure-based drug design led to analogues with improved potency and drug metabolism and pharmacokinetics properties.

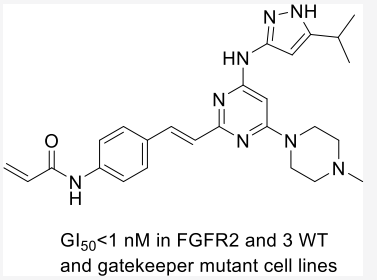

KEYWORDS: *FGFR, FGFR2, FGFR3, kinase inhibitor, gatekeeper mutant, RTK*

Aberrant signaling of the fibroblast growth factor receptor (FGFR) family of receptor tyrosine kinases (RTKs) has been shown to be a driver in a variety of tumors.[1−3] Enzymes in this family have emerged as promising targets for drug discovery, with numerous FGFR inhibitors entering the clinic in the past decade.[4−6] The recent approvals of erdafitinib (**1**) in FGFR3-aberrant bladder cancer[7,8] and pemigatinib (**2**) in FGFR2-aberrant cholangiocarcinoma[9,10] have clinically validated FGFR as a quality target for drug development. Numerous other FGFR and pan-RTK inhibitors are entering late stage clinical trials targeting tumors with FGFR activating mutations or fusions, including futibatinib (**3**)[11,12] and infigratinib (**4**).[13,14]

A common issue with RTK inhibition as a therapeutic mode is the development of resistance mutations in the tumors, leading to eventual disease recurrence.[15,16] The most common resistance mechanism to RTK inhibitors is the gatekeeper mutation, where a bulkier amino acid side chain "blocks" access to the back pocket of the kinase, a hydrophobic selectivity pocket that many RTK inhibitors take advantage of to gain potency and selectivity. Most first and second generation FGFR inhibitors take advantage of this back pocket, often using a functionalized dimethoxyphenyl ring (highlighted in red in Figure 1) to gain FGFR selectivity and enhance overall potency of the binders. While this has been a successful strategy, it leaves these inhibitors susceptible to acquired resistance through gatekeeper mutations, some of which are starting to arise in clinical samples.[17]

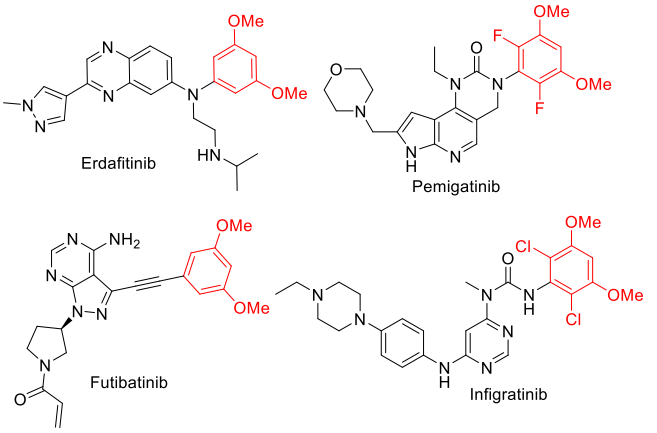

Figure 1. Some approved and clinical FGFR inhibitors.

Many second and third generation RTK inhibitor programs are centered on overcoming gatekeeper resistance while attempting to maintain potency and selectivity against the wild-type version of the kinase.[18,19] The aim of our next

Received: September 25, 2020
Accepted: November 25, 2020

generation FGFR inhibitor program was to identify and develop a series of inhibitors with activity against both wild-type and gatekeeper mutant variants of the FGFR2 and FGFR3 kinases. The most clinically relevant gatekeeper mutants are FGFR2-V564F and FGFR3-V555M. To overcome the potential loss of potency and kinase selectivity from avoiding the backpocket of the kinase, we intended to covalently target the P-loop cysteine that is conserved in all four isoforms of FGFR but is only present in five other human kinases.[20]

Our endeavor started with a targeted high-throughput screen using a deck of ∼10 000 compounds enriched with known hinge binders. The compounds were screened at a single concentration of 10 μM in a FRET assay using the FGFR3 V555M gatekeeper mutant protein. IC_{50} curves were generated for all "hit" molecules, followed by screening in cellular BaF3 lines engineered for sensitivity toward inhibition of wild-type and V555M FGFR3. This screening funnel produced a number of interesting "hit" compounds including compound **1** (Figure 2), which had sub-micromolar potency against both wild-type

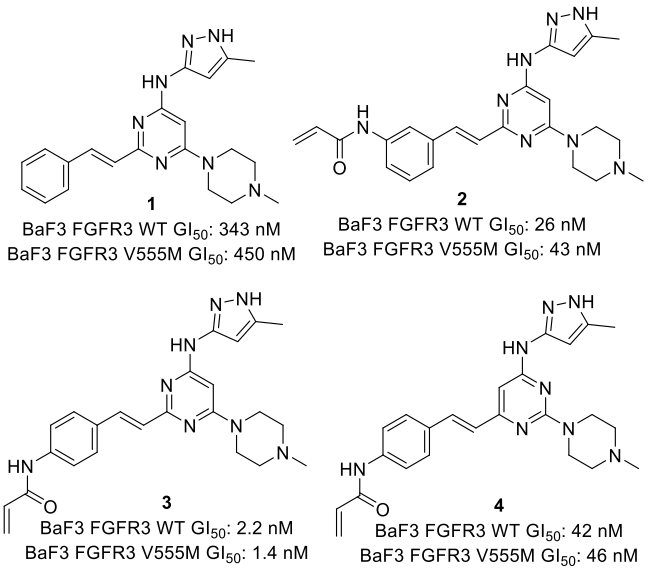

Figure 2. Initial lead compounds.

and mutant FGFR3 in cells. Compound **1** is a known Aurora kinase A inhibitor with some reported activity against wild-type FGFR3.[21] After computational docking of the hit into a known FGFR2 X-ray structure (PDB code 4RWKB, Figure 3), we added acrylamide electrophiles to the phenyl ring so that they

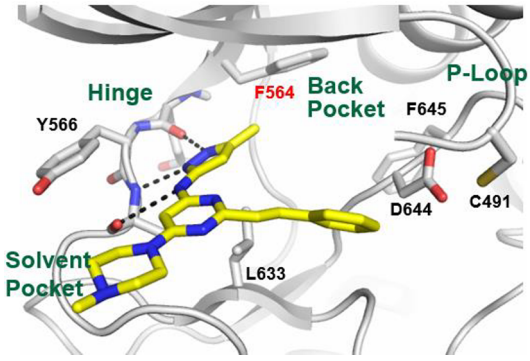

Figure 3. Docking model of compound **1** in FGFR2 V564F.

were properly aligned to potentially interact with the cysteine on the flexible P-loop of the kinase. Addition of an acrylamide to the *meta* (compound **2**, Figure 2) and *para* (**3**) positions of the phenyl ring gave dramatic boosts in potency, with compound **3** exhibiting single-digit nanomolar activity in both the wild-type and gatekeeper mutant FGFR3 cell lines. This compound immediately became the lead molecule for the program and was pushed forward into hit-to-lead optimization. Interestingly, the isomer of the pyrimidine was key to potency, and switching the position of one nitrogen (**4**) led to a substantial potency loss. This observation is probably due to steric repulsion between the C−H proton on the pyrimidine and the C−H proton on the pyrazole that keeps the molecule from adopting the ideal orientation to both bind the hinge and covalently modify the P-loop cysteine.

To further optimize compound **3**, we obtained an X-ray crystal structure in FGFR2 V564F (Figure 4), which showed

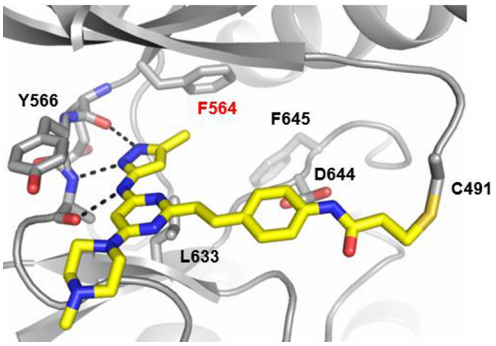

Figure 4. X-ray structure of compound **3** in FGFR2 V564F (PDB code 7KIE).

good density except for the acrylamide/P-loop, confirming that this part of the molecule is very flexible. Mass spectroscopy experiments confirmed that **3** covalently modified the protein (see the Supporting Information for details). Further optimization of compound **3** started with changes to the pyrazole hinge binder after analysis of the crystal structure revealed a small lipophilic pocket where we could gain additional potency without entering the back pocket and losing activity against the gatekeeper mutant. Small changes to the methyl group at the 5-position of the pyrazole could give a boost in potency (Table 1). The most potent group was the isopropyl in compound **6**, although other small aliphatic groups and ethers were also tolerated. We also explored some alternative hinge binders and found that thiazoles and imidazoles also gave single-digit nanomolar potency against both wild-type and gatekeeper mutant FGFR3. The polarized C−H bonds in these heterocycles can act as hydrogen bond donors that make hinge interactions similar to those observed in the pyrazole N−H. Synthesis of all of the compounds was straightforward, using selective couplings (Buchwald, Suzuki, SNAr) to commercially available 2,4,6-trichloropyrimidine (see the Supporting Information for synthetic details).

Compound **6** had potency against wild-type FGFR3 similar to the most potent reported FGFR inhibitors[22] while retaining sub-nanomolar potency against the gatekeeper mutant. Accordingly, it was further profiled in our testing cascade including *in vitro* drug metabolism and pharmacokinetics (DMPK) assays. Compound **6** showed sub-nanomolar potency against BaF3 FGFR2 WT and V564F gatekeeper mutant cell

https://dx.doi.org/10.1021/acsmedchemlett.0c00517
ACS Med. Chem. Lett. XXXX, XXX, XXX−XXX

Table 1. Optimization of the Hinge Binder

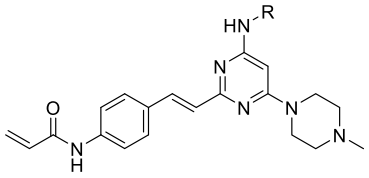

Cmp. #	R	BaF3 FGFR3 WT GI_{50} (nM)[a]	BaF3 FGFR3 V555M GI_{50} (nM)[a]
5	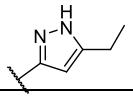	1.1	0.2
6	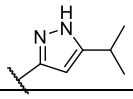	0.3	0.1
7	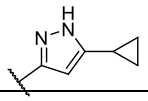	4.0	0.6
8	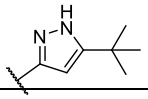	3.0	0.7
9	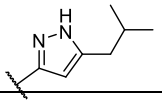	0.6	0.6
10	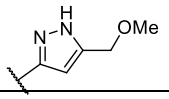	3.4	1.3
11	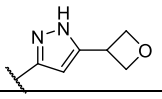	5.8	0.6
12	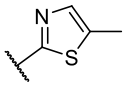	1.2	0.7
13	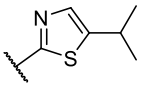	1.2	0.5
14	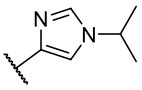	7.3	4.9

[a]All cellular assay data reported as an average of a minimum of two runs.

lines and single digit nanomolar activity against the RT112 cell line containing an endogenous FGFR3-TACC3 fusion (Table 2). Like most FGFR inhibitors, compound **6** retained activity against FGFR1, while showing some selectivity against FGFR4. While the potency was excellent across the board, the overall profile of this lead needed some improvement. Caco-2 permeability was low, while solubility and stability in mouse and human liver microsomes were moderate. The bigger concern was the stability in human and mouse whole blood,

Table 2. Profile of Compound 6

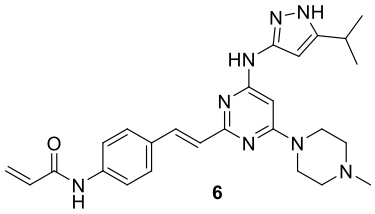

6

assay	result
FRFR2 V564F FRET IC_{50} (nM)	1.7
FRFR3 V555 M FRET IC_{50} (nM)	1.0
BaF3 FGFR2 WT GI_{50} (nM)	0.1
BaF3 FGFR2 V564F GI_{50} (nM)	0.1
RT112 GI_{50} (nM)	9.4
BaF3 FGFR1/4 GI_{50} (nM)	0.3/6.4
Caco2 A→B (10^{-6} cm/s)	0.1
blood stability hu/mu ($t_{1/2}$, min)	121/114
MLM/HLM CLint (μL/min/mg)	65/35
kinetic solubility (μM)	43
mouse CLtotal (mL/min/kg)[a]	86.3
mouse Vss (L/kg)[a]	3.1
mouse %F[b]	21
mouse PO Cmax (ng/mL)[b]	103
mouse PK PO AUC_obs (ng[a]h/mL)[b]	400

[a]CD-1 male mouse PK dosed IV at 5 mg/kg (formulation: 20% HP-β-CD in DI water). [b]Dosed PO at 10 mg/kg (formulation: 0.1% Tween and 0.5% CMC in water).

which was low, suggesting that the acrylamide electrophile was likely susceptible to addition of glutathione or other nucleophiles present in human and murine whole blood.[23] Compound **6** was run in mouse PK to establish a baseline for the program. As expected from the *in vitro* DMPK data, the clearance was high while oral bioavailability was moderate. This reinforced the need to improve metabolism and permeability to improve PK.

Follow-up compounds to **6** focused on improving metabolic stability while maintaining the excellent potency against both the wild-type and gatekeeper mutant variants of FGFR2 and 3. Therefore, we explored changes in the linker to the P-loop and the acrylamide electrophile (Table 3). We envisioned that such changes might also mitigate the susceptibility of the acrylamide to whole blood deactivation. For the linker, we were looking to move away from the olefin/aromatic system, which was presumed as a potential metabolic liability. For the electrophile, we wanted to explore nonaniline based functionalities to lower the reactivity of the electrophile.

Saturating the olefin (**15**) led to a substantial loss in potency, suggesting that a rigid linker was important to maintain activity. Using a known phenyl bioisostere in **16** also led to a significant potency drop but also to a significant improvement in whole blood and microsomal stability, indicating the culpability of the aniline acrylamide as our major metabolic liability. A series of nitrogen-containing heterocycles linked to the core by a phenyl ring were also profiled (**17**−**19**). While the azetidine (**17**) and pyrrolidine (**18**) were more potent, the piperidine (**19**) showed the most promising *in vitro* DMPK profile. Attempts to improve the potency of **19** by adding small lipophilic (**20**) or polar (**21**) groups to the pyrazole surprisingly gave a minimal boost in potency. Further attempts to optimize the linker to the P-loop included a variety of sp^3-rich linked and spirocyclic hetero-

https://dx.doi.org/10.1021/acsmedchemlett.0c00517
ACS Med. Chem. Lett. XXXX, XXX, XXX−XXX

Table 3. Optimization of Linker to the P-Loop

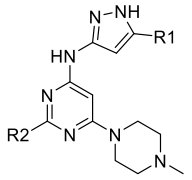

Cmp #	R1	R2	BaF3 FGFR3 WT GI_{50} (nM)	BaF3 FGFR3 V555M GI_{50} (nM)	BaF3 FGFR2 V564F GI_{50} (nM)	Caco2 A→B (10^{-6} cm/s)	HLM/MLM CLint (μL/min/mg protein)	Blood Stability hu/mu $t_{1/2}$ (min)
15	Me	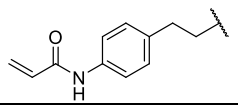	55	66	ND	0.3	23/52	247/157
16	Me	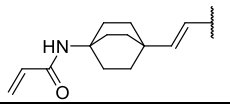	158	40	ND	0.7	13/15	>360/>360
17	Me	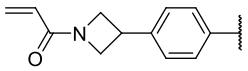	16	9.3	4.0	1.1	12/20	117/35
18[a]	Me	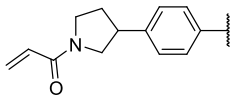	20	5.2	2.9	0.4	22/35	107/54
19	Me	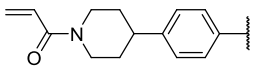	46	19	11	2.5	17/36	>360/259
20	iPr	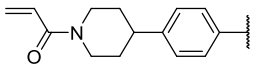	43	11	0.6	1.1	18/79	>360/>360
21		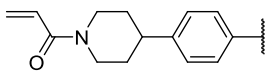	63	11	0.7	0.2	22/50	>360/>360
22	iPr	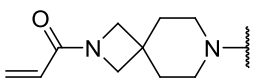	10	8.0	1.3	0.2	14/21	122/114
23	iPr	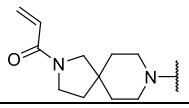	11	6.9	0.9	0.2	8.7/81	182/164
24[a]	iPr	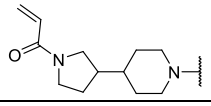	10	3.1	0.3	0.2	18/117	>360/350

[a]Data reported for racemic compound.

cycles (**22**−**24**). Many of these compounds had reasonable potency and improved blood and/or microsomal stability compared to the original lead, although Caco-2 permeability from apical-to-basolateral was a persistent issue.

Compound **19** showed the most promising combination of potency and DMPK profile, so it was further profiled and carried forward into mouse PK studies (Table 4). This compound has modest potency across all cell lines profiled and

https://dx.doi.org/10.1021/acsmedchemlett.0c00517
ACS Med. Chem. Lett. XXXX, XXX, XXX−XXX

Table 4. Profile of Compound 19

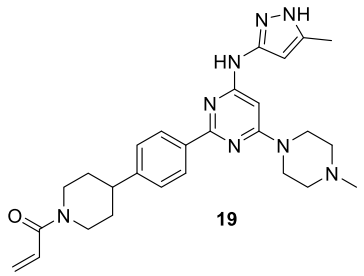

assay	result
FRFR2 V564F FRET IC_{50} (nM)	49
FRFR3 V555 M FRET IC_{50} (nM)	111
BaF3 FGFR2 WT GI_{50} (nM)	11.2
RT112 GI_{50} (nM)	52.9
BaF3 FGFR1/4 GI_{50} (nM)	25.1/438
BaF3 parental GI_{50} (nM)	2327
kinetic solubility (μM)	115
hepatocyte stability CLintmu/hu (μL/min/10^6 cells)	27/4.4
mouse CLtotal (mL/min/kg)[a]	53.6
mouse Vss (L/kg)[a]	2.0
mouse %F[b]	68
mouse PO Cmax (ng/mL)[b]	734
mouse PK PO AUC_obs (ng[a]h/mL)[b]	2100

[a]CD-1 Male Mouse PK dosed IV at 5 mg/kg (formulation: 20% HP-β-CD in DI water). [b]Dosed PO at 10 mg/kg (formulation: 0.1% Tween and 0.5% CMC in water).

some selectivity against FGFR4. A BaF3 parental cell line was used to assess general cytotoxicity, and while there was some activity, there was a significant window compared to the on-target lines. Dosing (**19**) via the IV route at a 5 mg/kg dose level showed moderate clearance, while an oral dose of 10 mg/kg displayed good bioavailability and oral exposure. The profile of (**19**) indicated that this series is amenable to optimization by demonstrating a reasonable *in vitro*/*in vivo* DMPK correlation. An X-ray crystal structure of **19** (Figure 5) was

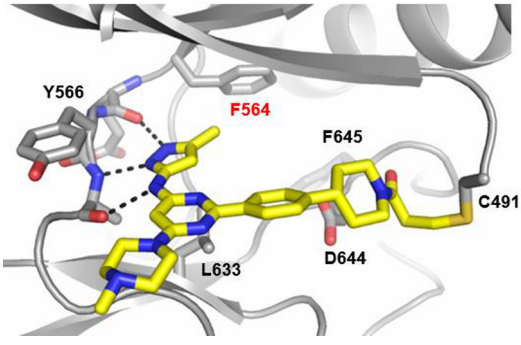

Figure 5. X-ray structure of compound **19** in FGFR2 V564F (PDB code 7KIA).

obtained, and it will be used for further modifications as we continue to search for the optimal balance between potency and PK in this series. Mass spectrometry analysis confirmed that the compound is covalently modifying the P-loop cysteine in FGFR.

A handful of the lead compounds were put into a DiscoverX mini-kinase panel to check binding to other kinases against which FGFR inhibitors have reported off-target activity (see the Supporting Information for details). Current work is looking at replacements for the methylpiperazine that can gain additional interactions around the solvent pocket and identification of any problematic off-target activity and further optimization of the linker to the P-loop to help find the optimal balance between potency and PK.

In conclusion, we have developed a series of novel 3-aminopyrazoles that show appreciable activity against both wild-type and gatekeeper mutant FGFR2 and 3 by utilizing covalent modification of a P-loop cysteine residue. Modifications of the linker that positions the electrophile in proximity to the P-loop has resulted in analogues with improved profiles that culminated in the identification of **19**. Current leading analogues seem to display similar *in vitro* wild-type activity to the current leading clinical FGFR2/3 inhibitors. Further work will focus on finding the appropriate balance between potency and DMPK properties in this series.

■ ASSOCIATED CONTENT

Supporting Information

The Supporting Information is available free of charge at https://pubs.acs.org/doi/10.1021/acsmedchemlett.0c00517.

Synthetic procedures, compound characterization, assay methods and conditions, and crystal structure data (PDF)

■ AUTHOR INFORMATION

Corresponding Author

Ryan A. Brawn − *H3 Biomedicine, Cambridge, Massachusetts 02139, United States;* orcid.org/0000-0003-0714-8182; Email: ryan_brawn@h3biomedicine.com

Authors

Andrew Cook − *H3 Biomedicine, Cambridge, Massachusetts 02139, United States*

Kiyoyuki Omoto − *H3 Biomedicine, Cambridge, Massachusetts 02139, United States*

Jiyuan Ke − *H3 Biomedicine, Cambridge, Massachusetts 02139, United States*

Craig Karr − *H3 Biomedicine, Cambridge, Massachusetts 02139, United States*

Federico Colombo − *H3 Biomedicine, Cambridge, Massachusetts 02139, United States*

Milena Virrankoski − *H3 Biomedicine, Cambridge, Massachusetts 02139, United States*

Sudeep Prajapati − *H3 Biomedicine, Cambridge, Massachusetts 02139, United States*

Dominic Reynolds − *H3 Biomedicine, Cambridge, Massachusetts 02139, United States*

David M. Bolduc − *H3 Biomedicine, Cambridge, Massachusetts 02139, United States;* orcid.org/0000-0003-2003-8631

Tuong-Vi Nguyen − *H3 Biomedicine, Cambridge, Massachusetts 02139, United States*

Patricia Gee − *H3 Biomedicine, Cambridge, Massachusetts 02139, United States*

Deanna Borrelli − *H3 Biomedicine, Cambridge, Massachusetts 02139, United States*

Benjamin Caleb − *H3 Biomedicine, Cambridge, Massachusetts 02139, United States*

Shihua Yao − *H3 Biomedicine, Cambridge, Massachusetts 02139, United States*

https://dx.doi.org/10.1021/acsmedchemlett.0c00517
ACS Med. Chem. Lett. XXXX, XXX, XXX−XXX

Sean Irwin − *H3 Biomedicine, Cambridge, Massachusetts 02139, United States*
Nicholas A. Larsen − *H3 Biomedicine, Cambridge, Massachusetts 02139, United States*
Anand Selvaraj − *H3 Biomedicine, Cambridge, Massachusetts 02139, United States*
Xuesong Zhao − *H3 Biomedicine, Cambridge, Massachusetts 02139, United States*
Stephanos Ioannidis − *H3 Biomedicine, Cambridge, Massachusetts 02139, United States*

Complete contact information is available at: https://pubs.acs.org/10.1021/acsmedchemlett.0c00517

Author Contributions

The manuscript was written through contributions of all authors. All authors have given approval to the final version of the manuscript.

Notes

The authors declare no competing financial interest.

■ ACKNOWLEDGMENTS

The authors would like to thank the H3 leadership team for supporting this publication and our co-workers for helpful discussions and advice.

■ ABBREVIATIONS

FGFR, fibroblast growth factor receptor; RTK, receptor tyrosine kinase; WT, wild-type; PDB, Protien Data Bank; FRET, fluorescence resonance energy transfer; nM, nanomolar; HLM, human liver microsomes; MLM, mouse liver microsomes; mu/hu, mouse/human; $t_{1/2}$, half-life; Cl_{int}, intrinsic clearance; μL, microliter; μM, micromolar; Cltotal, total clearance; Vss, volume of distribution; %F, percentage bioavailability; PO, oral dosing; Cmax, maximum concentration in blood; ng, nanograms; AUC_obs, observed area under the curve; HP-β-CD, beta-cyclodextrin; CMC, carboxymethylcellulose sodium

■ REFERENCES

(1) Katoh, M. Fibroblast growth receptors as treatment targets in clinical oncology. *Nat. Rev. Clin. Oncol.* **2019**, *16*, 105−122.
(2) Turner, N.; Grose, R. Fibroblast growth factor signaling: from development to cancer. *Nat. Rev. Cancer* **2010**, *10*, 116−129.
(3) Dieci, M. V.; Arnedos, M.; Andre, F.; Soria, J. C. Fibroblast growth factor receptor inhibitors as a cancer treatment: from a biologic rationale to medical perspectives. *Cancer Discovery* **2013**, *3*, 264−279.
(4) Babina, I. S.; Turner, N. C. Advances and Challenges in targeting FGFR signaling in cancer. *Nat. Rev. Cancer* **2017**, *17*, 318−332.
(5) Chae, Y. K.; Ranganath, K.; Hammerman, P. S.; Vaklavas, C.; Mohindra, N.; Kalyan, A.; Matsangou, M.; Costa, R.; Carneiro, B.; Villaflor, V. M.; Cristofanilli, M.; Giles, F. J. Inhibition of the fibroblast growth factor receptor (FGFR) pathway: the current landscape and barriers to clinical application. *Oncotarget* **2017**, *8*, 16052−16074.
(6) Carter, E. P.; Fearon, A. E.; Grose, R. P. Careless talk costs lives: fibroblast growth factor receptor signaling and the consequences of pathway malfunction. *Trends Cell Biol.* **2015**, *25*, 221−233.
(7) Perera, T. P. S.; Jovcheva, E.; Mevellec, L.; Vialard, J.; De Lange, D.; Verhulst, T.; Paulussen, C.; Van De Ven, K.; King, P.; Freyne, E.; Rees, D. C.; Squires, M.; Saxty, G.; Page, M.; Murray, C. W.; Gilissen, R.; Ward, G.; Thompson, N. T.; Newell, D. R.; Cheng, N.; Xie, L.; Yang, J.; Platero, S. J.; Karkera, J. D.; Moy, C.; Angibaud, P.; Laquerre, S.; Lorenzi, M. V. Discovery and pharmacological characterization of JNJ-42756493 (erdafitinib), a functionally selective small-molecule FGFR family inhibitor. *Mol. Cancer Ther.* **2017**, *16*, 1010−1020.
(8) Announcement from the Janssen website, April 12, 2019. https://www.janssen.com/balversa-erdafitinib-receives-us-fda-approval-treatment-patients-locally-advanced-or-metastatic.
(9) Liu, P. C. C.; Koblish, H.; Wu, L.; Bowman, K.; Diamond, S.; DiMatteo, D.; et al. INCB054828 (pemigatinib), a potent and selective inhibitor of fibroblast growth factor receptors 1, 2, and 3, displays activity against genetically defined tumor models. *PLoS One* **2020**, *15*, No. e0231877.
(10) Press release from the Incyte website, April 17, 2020. https://investor.incyte.com/press-releases/press-releases/2020/FDA-Approves-Incytes-Pemazyre-pemigatinib-as-First-Targeted-Treatment-for-Adults-with-Previously-Treated-Unresectable-Locally-Advanced-or-Metastatic-Cholangiocarcinoma/default.aspx.
(11) Ochiiwa, H.; Fujita, H.; Itoh, K.; Sootome, H.; Hashimoto, A.; Fujioka, Y.; Nakatsuru, Y.; Oda, N.; Yonekura, K.; Hirai, H.; Utsugi, T. TAS-120, a highly potent and selective irreversible FGFR inhibitor, is effective in tumors harboring various FGFR gene abnormalities. *Mol. Cancer Ther.* **2013**, *12*, A270.
(12) Clinical trial information, October 2020. https://clinicaltrials.gov/ct2/show/NCT02052778?term=TAS-120.
(13) Guagnano, V.; Furet, P.; Spanka, C.; Bordas, V.; Le Douget, M.; Stamm, C.; Brueggen, J.; Jensen, M. R.; Schnell, C.; Schmid, H.; Wartmann, M.; Berghausen, J.; Drueckes, P.; Zimmerlin, A.; Bussiere, D.; Murray, J.; Porta, D. G. Discovery of 3-(2,6-Dichloro-3,5-dimethoxy-phenyl)-1-{6-[4-(4-ethyl-piperazin-1-yl)-phenylamino]-pyrimidin-4-yl}-1-methyl-urea (NVP-BGJ398), A Potent and Selective Inhibitor of the Fibroblast Growth Factor Receptor Family of Receptor Tyrosine Kinase. *J. Med. Chem.* **2011**, *54*, 7066−7083.
(14) For current clinical trials (October 2020), see: https://www.clinicaltrials.gov/ct2/results?cond=&term=infigratinib&cntry=&state=&city=&dist=.
(15) Engelman, J. A; Settleman, J. Acquired resistance to tyrosine kinase inhibitors during cancer therapy. *Curr. Opin. Genet. Dev.* **2008**, *18*, 73−79.
(16) Alexander, P. B.; Wang, X.-F. Resistance to receptor tyrosine kinases in cancer: molecular mechanisms and therapeutic strategies. *Front. Med.* **2015**, *9*, 134−138.
(17) Goyal, L.; Saha, S. K.; Liu, L. Y.; Siravegna, G.; Leshchiner, I.; Ahronian, L. G.; et al. Polyclonal Secondary FGFR2 Mutations Drive Acquired Resistance to FGFR Inhibition in Patients with FGFR2 Fusion-Positive Cholangiocarcinoma. *Cancer Discovery* **2017**, *7*, 252−263.
(18) Guo, H.; Wan, Z.-K.; Qin, L.; Liu, Q.; Cheung, W. S. Second-Generation FGFR Inhibitors for the Treatment of Cancers Harboring Mutated FGFRs Patent application number WO 2019/101182A1.
(19) Lu, X.; Smaill, J. B.; Ding, K. Medicinal Chemistry Strategies for the Development of Kinase Inhibitors Targeting Point Mutations. *J. Med. Chem.* **2020**, *63*, 10726.
(20) Du, G.; Rao, S.; Gurbani, D.; Henning, N. J.; Jiang, J.; Che, J.; Yang, A.; Ficarro, S. B.; Marto, J. A.; Aguirre, A. J.; Sorger, P. K.; Westover, K. D.; Zhang, T.; Gray, N. S. Structure-Based Design of a Potent and Selective Covalent Inhibitor for SRC Kinase That Targets a P-Loop Cysteine. *J. Med. Chem.* **2020**, *63*, 1624−1641.
(21) Xiao, X.-Y.; Patel, D. V.; Ward, J. S.; Bray, M. R.; Agoston, G. E.; Treston, A. M. Substituted pyrazole compounds. United States patent US 7,563,787, September 29, 2006.
(22) Cheng, W.; Wang, M.; Tian, X.; Zhang, X. An overview of the binding models of FGFR tyrosine kinases in complex with small molecule inhibitors. *Eur. J. Med. Chem.* **2017**, *126*, 476−490.
(23) A significant amount of the potency in **6** was driven by the active electrophile; see the Supporting Information for the activity of the compound when the acrylamide is saturated.

https://dx.doi.org/10.1021/acsmedchemlett.0c00517
ACS Med. Chem. Lett. XXXX, XXX, XXX−XXX